Molecular Pharmacology Fast Forward. Published on December 23, 2015 as DOI: 10.1124/mol.115.101246
This article has not been copyedited and formatted. The final version may differ from this version.

A hydrogen-bonded polar network in the core of the glucagon-like peptide-1 receptor is a fulcrum for biased agonism: lessons from class B crystal structures.

Denise Wootten, Christopher A Reynolds, Cassandra Koole, Kevin J Smith, Juan C Mobarec, John Simms, Tezz Quon, Thomas Coudrat, Sebastian G. B. Furness, Laurence J Miller, Arthur Christopoulos, and Patrick M. Sexton

Monash Institute of Pharmaceutical Sciences and Department of Pharmacology, Monash University, Parkville 3052, Victoria, Australia (PMS, CK, TQ, TC, SGBF, AC, DW)

School of Biological Sciences, University of Essex, Wivenhoe Park, Colchester CO4 3SQ, U.K. (CAR, KJS, JCM)

Department of Molecular Pharmacology and Experimental Therapeutics, Mayo Clinic, Scottsdale, AZ 85259, U.S.A. (LJM)

School of Life and Health Sciences, Aston University, Birmingham B4 7ET, UK (JS)

Molecular Pharmacology Fast Forward. Published on December 23, 2015 as DOI: 10.1124/mol.115.101246
This article has not been copyedited and formatted. The final version may differ from this version.

MOL #101246

Running title: A GLP-1 receptor polar network for biased agonism

Address correspondence to:

Dr. Denise Wootten

Drug Discovery Biology

Monash Institute of Pharmaceutical Sciences

Monash University

381 Royal Parade, Parkville, Victoria 3052.

Australia

Email: denise.wootten@monash.edu; Phone: +613 9903 9088

Or

Prof. Patrick Sexton

Drug Discovery Biology

Monash Institute of Pharmaceutical Sciences

Monash University

381 Royal Parade, Parkville, Victoria 3052.

Australia

Email: patrick.sexton@monash.edu; Phone: +613 9903 9069

Text pages: 40

Number of tables: 3

Number of figures: 7

Number of references: 51

Number of words in Abstract: 238

Number of words in Introduction: 737

Number of words in Discussion: 1828

Molecular Pharmacology Fast Forward. Published on December 23, 2015 as DOI: 10.1124/mol.115.101246
This article has not been copyedited and formatted. The final version may differ from this version.

Abbreviations:

CHO, Chinese hamster ovary; CRF1, corticotropin releasing factor 1; DMEM, Dulbecco's modified Eagle medium; ERK, extracellular signal-regulated kinase; FBS, fetal bovine serum; GLP-1, glucagon-like peptide-1; GPCR, G protein-coupled receptor; MD, molecular dynamics; PBS, phosphate buffered saline; POPC, 1-palmitoyl-2-oleoyl-sn-glycero-3-phosphocholine; TM, transmembrane helix.

Molecular Pharmacology Fast Forward. Published on December 23, 2015 as DOI: 10.1124/mol.115.101246
This article has not been copyedited and formatted. The final version may differ from this version.

Abstract

The glucagon-like peptide 1 (GLP-1) receptor is a class B G protein-coupled receptor (GPCR) that is a key target for treatments for type II diabetes and obesity. This receptor, like other class B GPCRs, displays biased agonism, though the physiological significance of this is yet to be elucidated. Previous work has implicated R2.60^{190}, N3.43^{240}, Q7.49^{394} and H6.52^{363} as key residues involved in peptide-mediated biased agonism (Wootten et al., 2013a), with R2.60^{190}, N3.43^{240} and Q7.49^{394} predicted to form a polar interaction network. In this study, we used novel insight gained from recent crystal structures of the transmembrane domains of the glucagon and corticotropin releasing factor 1 (CRF1) receptors to develop improved models of the GLP-1 receptor that predict additional key molecular interactions with these amino acids. We have introduced E6.53^{364}A, N3.43^{240}Q, Q7.49^{394}N and N3.43^{240}Q/ Q7.49^{394}N mutations to probe the role of predicted H-bonding and charge-charge interactions in driving cAMP, calcium or ERK signaling. A polar interaction between E6.53^{364} and R2.60^{190} was predicted to be important for GLP-1- and exendin-4-, but not oxyntomodulin-mediated cAMP formation and also ERK1/2 phosphorylation. In contrast, Q7.49^{394}, but not R2.60^{190}/ E6.53^{364} was critical for calcium mobilisation for all three peptides. Mutation of N3.43^{240} and Q7.49^{394} had differential effects on individual peptides providing evidence for molecular differences in activation transition. Collectively, this work expands our understanding of peptide-mediated signaling from the GLP-1 receptor and the key role that the central polar network plays in these events.

Molecular Pharmacology Fast Forward. Published on December 23, 2015 as DOI: 10.1124/mol.115.101246
This article has not been copyedited and formatted. The final version may differ from this version.

Introduction

Glucagon-like peptide 1 (GLP-1) is a key incretin hormone controlling insulin secretion in response to meal ingestion that has a broad range of actions potentially beneficial for treatment of type II diabetes and obesity. These include promotion of insulin synthesis and release, decreased glucagon production, preservation of pancreatic β-cell mass, decreased appetite and gastric empyting and preservation and promotion of cardiac function (reviewed in Koole et al., 2013; Baggio and Drucker, 2007; Pabreja et al., 2014). GLP-1 acts via the GLP-1 receptor, a class B peptide hormone G protein-coupled receptor (GPCR). This class includes receptors for many important peptides including parathyroid hormone, secretin, calcitonin, amylin, vasoactive intestinal polypeptide, corticotropin-releasing hormone (CRF), gastric inhibitory peptide, glucagon, as well as the glucagon-like peptides (Hollenstein et al., 2014). As such, understanding of how these peptides bind to and activate their cognate receptors is critical to understanding their action and to unlocking the therapeutic potential of targeting this receptor class.

The revolution in membrane protein crystallography and GPCR structural biology has generated novel insight into our understanding of the structural basis for receptor activation, including the importance of structural waters and polar, hydrogen bond networks for propagation of the conformational rearrangements required for receptor activation and coupling of the receptor to effector proteins (Caltabiano et al., 2013; Katrich et al., 2014). Many of these key networks are conserved within subfamilies of class A GPCRs (Venkatakrishnan et al., 2013). It is also increasingly recognised that individual ligands acting at the same GPCR can elicit distinct profiles of signaling and regulation, a phenomenon termed biased agonism (Shonberg et al., 2014). At a molecular level this occurs through the distinct interactions that individual ligands make with their target receptor and the potential

Molecular Pharmacology Fast Forward. Published on December 23, 2015 as DOI: 10.1124/mol.115.101246
This article has not been copyedited and formatted. The final version may differ from this version.

for these interactions to stabilise distinct conformational ensembles that in turn favour differential interaction with effector proteins (Shonberg et al., 2014). How these distinct interactions drive conformational propagation is still poorly understood, but it is hypothesised to involve selective recruitment of structurally important interaction networks.

Less is understood about the activation of class B peptide GPCRs as they do not contain the key conserved amino acids that are signatures of class A receptors and critical for their function. Nonetheless, class B GPCRs have their own unique set of conserved, intramembranous, polar residues that are likely comparable to those in class A. Prototypic of this receptor class is the GLP-1 receptor that displays pleiotropic coupling and both peptide and non-peptidic biased agonism (Koole et al., 2010; Wootten et al., 2013b; Willard et al., 2013; Weston et al., 2014; Jorgensen et al., 2007; Coopman et al., 2010; Cheong et al., 2012). Recently, the role of the conserved intramembranous polar residues in this receptor was probed by alanine scanning mutagenesis, which revealed clusters of amino acids important for a range of functions including protein expression, and the control of activation transition for both general signal pathway bias and ligand-directed biased signaling (Wootten et al., 2013a). A key network for differential effects on peptide-mediated signaling for GLP-1, exendin-4 and oxyntomodulin was identified that involved R2.60^{190}, N3.43^{240}, H6.52^{363} and Q7.49^{394} (Wootten et al., 2013a numbering scheme, amino acid numbers are shown in superscript). Using an early model of the GLP-1 receptor, it was predicted that the R2.60^{190} coordinated interactions with the Asn and Gln and that these interactions were differentially important for signaling via the individual peptides. Nonetheless, double mutation of Asn3.43^{240} and Gln7.49^{394} did not fully recapitulate the phenotype of the Arg2.60^{190} mutation (Wootten et al., 2013a) suggesting that the model was insufficient to fully explain the differential effects on signaling.

Molecular Pharmacology Fast Forward. Published on December 23, 2015 as DOI: 10.1124/mol.115.101246
This article has not been copyedited and formatted. The final version may differ from this version.

Recently, transmembrane crystal structures of the glucagon and CRF1 receptors were solved (Siu et al., 2013; Hollenstein et al., 2013). These revealed that the class B GPCRs have distinct arrangements of the transmembrane bundle compared to class A GPCRs, leading to a large, solvent exposed, V-shaped extracellular-facing cavity that is likely critical for peptide-mediated receptor activation. These distinctions contribute to the historic difficulty in modelling of class B receptors. The new structural data revealed that our original GLP-1 receptor model used to interpret data on polar residue mutants was inaccurate, although the predicted interactions between $R^{2.60}$, $N3.43^{240}$ and $Q7.49^{394}$ were maintained.

To gain further insight into the role of the predicted network, we have generated new GLP-1 receptor models based on the available crystal structures and performed additional mutagenesis to probe the nature and importance of this network for peptide-mediated activation of key signaling pathways.

Molecular Pharmacology Fast Forward. Published on December 23, 2015 as DOI: 10.1124/mol.115.101246
This article has not been copyedited and formatted. The final version may differ from this version.

Materials and Methods

Materials. Dulbecco's Modified Eagle Medium (DMEM), hygromycin-B, and Fluo-4 acetoxymethyl ester were purchased from Invitrogen (Carlsbad, CA, USA). Fetal Bovine Serum (FBS) was purchased from Thermo Fisher Scientific (Melbourne, VIC, Australia). The QuikChange site-directed mutagenesis kit was purchased from Stratagene (La Jolla, CA, USA). AlphaScreen™ reagents, Bolton-Hunter reagent [^{125}I], and 384-well ProxiPlates were purchased from PerkinElmer Life and Analytical Sciences (Waltham, MA, USA). SureFire™ pERK1/2 reagents were generously supplied by TGR Biosciences (Adelaide, SA, Australia). SigmaFast *o*-phenylenediamine dihydrochloride tablets and antibodies were purchased from Sigma-Aldrich (St. Louis, MO, USA). GLP-1 peptides were purchased from American Peptide (Sunnyvale, CA, USA). All other reagents were purchased from Sigma-Aldrich (St. Louis, MO, USA) or BDH Merck (Melbourne, VIC, Australia) and were of an analytical grade.

Receptor Mutagenesis. The desired mutations were introduced to an N-terminally double c-myc labeled wildtype human GLP-1 receptor (GLP-1 receptor) in the pEF5/FRT/V5-DEST destination vector (Invitrogen); this receptor had pharmacology equivalent to the untagged human GLP-1 receptor (data not shown). Mutagenesis was carried out using oligonucleotides for site-directed mutagenesis purchased from GeneWorks and the QuikChange site-directed mutagenesis kit (Stratagene), and confirmed by automated sequencing.

Transfections and Cell Culture. Wildtype and mutant human GLP-1 receptor were isogenically integrated into FlpIn-Chinese hamster ovary (FlpInCHO) cells (Invitrogen) and selection of receptor-expressing cells accomplished by treatment with 600 μg/mL

Molecular Pharmacology Fast Forward. Published on December 23, 2015 as DOI: 10.1124/mol.115.101246
This article has not been copyedited and formatted. The final version may differ from this version.

hygromycin-B. Transfected and parental FlpInCHO cells were maintained in DMEM supplemented with 10% (v/v) heat-inactivated FBS and incubated in a humidified environment at 37 °C in 5% CO_2. Whenever a new series of mutant receptors is generated and used for generation of stable cell lines, the cells used for the specific set of transfections are used to generate a new wild-type receptor control, to account for any drift in cell background with change of passage. Experiments on mutant receptors are run in parallel with these controls. Where data from wild-types from different series of experiments was equivalent, this data was pooled.

Radioligand Binding Assay. FlpInCHO wildtype and mutant human GLP-1 receptor cells were seeded at a density of 3 x 10^4 cells per well into 96-well culture plates and incubated overnight at 37 °C in 5% CO_2, and radioligand binding carried out as previously described (Koole et al., 2011). For each cell line in all experiments, total binding was defined by ~0.05 nM [^{125}I]exendin(9–39) alone, and nonspecific binding was determined in the presence of 1 μM exendin(9–39). For analysis, data are normalised to the specific binding for each individual experiment.

cAMP Accumulation Assay. FlpInCHO wildtype and mutant human GLP-1 receptor cells were seeded at a density of 3 x 10^4 cells per well into 96-well culture plates and incubated overnight at 37 °C in 5% CO_2, and cAMP detection was carried out as previously described (Koole et al., 2010). All values were converted to concentration of cAMP using a cAMP standard curve performed in parallel, and data were subsequently normalised to the response of 100 μM forskolin in each cell line.

Molecular Pharmacology Fast Forward. Published on December 23, 2015 as DOI: 10.1124/mol.115.101246
This article has not been copyedited and formatted. The final version may differ from this version.

pERK 1/2 Assay. FlpInCHO wildtype and mutant human GLP-1 receptor cells were seeded at a density of 3 x 10^4 cells per well into 96-well culture plates and incubated overnight at 37 °C in 5% CO_2. Receptor-mediated pERK1/2 was determined using the AlphaScreen™ pERK1/2 SureFire™ protocol as previously described (Koole et al., 2010). Initial pERK1/2 time course experiments were performed over 1 h to determine the time at which agonist-mediated pERK1/2 was maximal. Subsequent experiments were then performed at the time required to generate a maximal pERK1/2 response (6 min). Data were normalised to the maximal response elicited by 10% (v/v) FBS in each cell line, determined at 6 min (peak FBS response).

$_iCa^{2+}$ Mobilisation Assay. FlpInCHO wildtype and mutant human GLP-1 receptor cells were seeded at a density of 3 x 10^4 cells per well into 96-well culture plates and incubated overnight at 37 °C in 5% CO_2, and receptor-mediated $_iCa^{2+}$ mobilisation was determined as previously described (Koole et al., 2010). Fluorescence was determined immediately after peptide addition, with an excitation wavelength set to 485 nm and an emission wavelength set to 520 nm, and readings were taken every 1.36 s for 120 s. Peak magnitude was calculated using five-point smoothing, followed by correction against basal fluorescence. The peak value was used to create concentration-response curves. Data were normalised to the maximal response elicited by 100 μM ATP, and to the WT receptor responses.

Cell-Surface Receptor Expression. FlpInCHO wildtype and mutant human GLP-1 receptor cells, with receptor DNA previously incorporated with an N-terminal double c-myc epitope label, were seeded at a density of 25 x 10^4 cells per well into 24-well culture plates and incubated overnight at 37 °C in 5% CO_2, washed three times in 1 x PBS, and fixed with 3.7% (v/v) paraformaldehyde at 4 °C for 15 min. Cell-surface receptor detection was then

Molecular Pharmacology Fast Forward. Published on December 23, 2015 as DOI: 10.1124/mol.115.101246
This article has not been copyedited and formatted. The final version may differ from this version.

performed as previously described (Koole et al., 2011). Data were normalised to the basal fluorescence detected in FlpInCHO parental cells. Specific [^{125}I]exendin(9–39) binding at each receptor mutant, as identification of functional receptors at the cell surface, was also determined [corrected for nonspecific binding using 1 μM exendin (9–39)].

Data Analysis. All data were analysed using Prism 6.0 (GraphPad Software Inc., San Diego, CA, USA). For all analyses the data were unweighted and each *y* value (mean of replicates for each individual experiment) was considered an individual point. Concentration response signaling data were analysed using a three-parameter logistic equation as previously described (May et al., 2007):

$$Y = Bottom + \frac{(Top - Bottom)}{1 + 10^{(LogEC_{50} - log[A])}} \quad (1)$$

where *Bottom* represents the *y* value in the absence of ligand(s), *Top* represents the maximal stimulation in the presence of ligand(s), [*A*] is the molar concentration of ligand, and EC_{50} represents the molar concentration of ligand required to generate a response halfway between *Top* and *Bottom*. Similarly, this equation was used in the analysis of inhibition binding data, instead replacing EC_{50} with IC_{50}. In this case, *Bottom* defines the specific binding of the radioligand that is equivalent to non-specific ligand binding, whereas *Top* defines radioligand binding in the absence of a competing ligand, and the IC_{50} value represents the molar concentration of ligand required to generate an effect halfway between *Top* and *Bottom*.

To quantify efficacy in the system, all data were fitted with an operational model of agonism (Black and Leff, 1983):

$$Y = Bottom + \frac{E_m - Bottom}{1 + ((10^{logK_A}) + (10^{log[A]}))/(10^{(log\tau + log[A])})} \quad (2)$$

Molecular Pharmacology Fast Forward. Published on December 23, 2015 as DOI: 10.1124/mol.115.101246
This article has not been copyedited and formatted. The final version may differ from this version.

where E_m represents the maximal stimulation in the system; K_A is the agonist-receptor functional dissociation constant, in molar concentration, that is dependent upon the receptor-effector complex driving signalling for an individual pathway (Kenakin et al., 2012; Kenakin and Christopoulos, 2013); τ is the estimated measure of efficacy in the system, which incorporates both signaling efficacy and receptor density; and all other parameters are as defined for Equation 1. Constraints for this model were determined by fitting the most efficacious peptide with the following equation:

(3) $$Y = Bottom + \frac{E_m - Bottom}{1 + 10^{(LogEC_{50}-log[A])}}$$

The value obtained for the system maximum (E_m) was then globally constrained in the operational model (Equation 2) when applied at each mutant receptor. All estimated τ values were then corrected to cell surface expression (τ_c); Bmax from homologous competition (equation 4) of ^{125}I-exendin(9-39) binding by unlabelled exendin(9-39) where Bmax is the maximum binding of ligand to receptors, [Hot] is the concentration of ^{125}I-exendin(9-39) in nM, [Cold] is the concentration of unlabelled exendin(9-39) in nM, and Kd is the equilibrium dissociation constant of the ligand in nM, with Bottom as defined in equation 1. Errors were propagated from both τ and cell surface expression relative to wildtype receptor.

(4) $$Y = \frac{Bmax\ x\ [Hot]}{[Hot]+[Cold]+Kd} + Bottom$$

Statistics. Changes in peptide affinity, potency, efficacy, and cell surface expression of human GLP-1 receptor mutants in comparison to wildtype human GLP-1 receptor control

Molecular Pharmacology Fast Forward. Published on December 23, 2015 as DOI: 10.1124/mol.115.101246
This article has not been copyedited and formatted. The final version may differ from this version.

were statistically analysed with one-way analysis of variance and Dunnett's post-test, and significance accepted at $p < 0.05$.

Molecular Modeling.

The apo GLP-1R model of the TM domain (Data Supplement 1) was generated from the glucagon X-ray crystal structure (Siu et al., 2013) using the homology modeling and minimization facilities of PLOP (Jacobson et al., 2004). The full GLP-1-bound GLP-1R used additional templates, namely the X-ray structure of the ECD with GLP-1(10-35) bound (Underwood et al., 2010), the CRF-R1 X-ray structure (used to model ECL1, which is missing in the glucagon structure) (Hollenstein et al., 2013) and the NMR structure of a conformationally constrained GLP-1(7-17) analogue (Hoang et al., 2015) docked to a GLP-1R model (pre-primed to bind GLP-1 using Modeller; Eswar et al., 2007) using GLIDE (v6.9) SP peptide and the OPLS 3.0 force field (Tubert-Brohman et al., 2013; Friesner et al., 2004). A 20×20×20 $Å^3$ inner docking box and a 44×44×44 $Å^3$ outer docking box centred at the opening of the TM bundle was used; the peptide backbone was held rigid during the docking. GLP-1(7-17)NH_2 generated from model 7 from the NMR ensemble, pdb code 2N0I, using PLOP gave the highest scoring docked pose. Because this analogue had similar activity to GLP-1(7-36)NH_2 and was conformationally constrained (Hoang et al., 2015), it provided the best currently available model for the conformation of GLP-1. In addition, the X-ray structure of the C-terminal peptide of the G-protein alpha subunit (R373-L394) in complex with the intracellular part and TM5 and TM6 of the β_2-adrenergic receptor from the X-ray structure of the receptor:G-protein complex (Rasmussen et al., 2011) (mutated to its GLP-1R equivalent using Modeller) was used as an additional template to facilitate generation of an active model. The success of the comparative modeling required a reasonable structural overlap between the TM region and the ECD region and for this reason GLP-1(7-36)NH_2 was structurally aligned

Molecular Pharmacology Fast Forward. Published on December 23, 2015 as DOI: 10.1124/mol.115.101246
This article has not been copyedited and formatted. The final version may differ from this version.

to GLP-1(10-35) of the ECD complex using VMD (Humphrey et al., 1996) to generate an ECD complex containing GLP-1(7-35). These templates were linked by a global alignment, which was used by Modeller to generate a full GLP-1R model with GLP-1(7-36)NH_2 bound. Modeller used 4 Bpa photoaffinity crosslinking-derived distance constraints between GLP-1 and GLP-1R (Chen et al., 2009; 2010; Miller et al., 2011) and two sets of constraints derived from reciprocal mutagenesis experiments that resulted in gain of function (Moon et al., 2015; Vertongen et al., 2001; Solano et al., 2001), as shown in Table 1; the effect of these constraints was to provide additional information on the peptide-receptor interaction in the region between the TM and ECD templates. These reciprocal mutagenesis results were essentially the only mutagenesis results used in the generation of the model. Two thousand models were generated by Modeller and the model with the best (lowest) DOPE score was selected. This model was subjected to further refinement of ECL1 using a template derived from the CRF-R1 structure and the additional constraints given in Supplemental Table 1, with the final model selected as having the best DOPE score from 5000 models. The structures are available from ftp://ftp.essex.ac.uk/pub/oyster/Wootten_GLP-1R_2015/ (username: ftp, password: anonymous; Data Supplement 2). Molecular dynamics (MD) simulations were carried out using fully hydrated models in a POPC bilayer using ACEMD (Harvey et al., 2009), with parameters taken from the AMBER 14SB (Hornak et al., 2006) and lipid 14 force fields (Walker et al., 2014); the apo model for MD was generated by removing the ligand and run for 240 ns.

Hydration of the glucagon receptor transmembrane domain crystal structure was predicted using the Sample Flood algorithm within the ICM package (Molsoft, San Diego).

Molecular Pharmacology Fast Forward. Published on December 23, 2015 as DOI: 10.1124/mol.115.101246
This article has not been copyedited and formatted. The final version may differ from this version.

Results

In this paper, we have generated a homology model of the apo form of the GLP-1 receptor transmembrane domain based on the inactive glucagon receptor TM crystal structure. Although marked distinction in the upper regions of the receptor occurred relative to our previously reported model (Wootten et al., 2013a), the key interaction network co-ordinated by R2.60^{190}, predicted in initial modelling, was maintained (Figure 1B, E). Nonetheless, there were substantial differences in the position of TM6 with a rotation and an outward translocation of the extracellular end of the helix that contributes to the opening of the extracellular face of the receptor, and also in the positioning of TM5 that is translocated two helical turns towards the intracellular face of the receptor (Figure 1A, B). This latter difference positions N5.50^{320} much deeper into the membrane. The rotation of TM6 moves H6.52^{363} away from the core of the transmembrane domain bundle and E6.53^{364} into the core (Figure 1A, B, E). Collectively, the new modelling predicts that key residues involved in receptor-mediated signaling bias, both those involved in peptide-mediated bias and those involved globally in altering signaling bias for all peptides (Wootten et al., 2013a) are co-located in the mid-region of the helical bundle (Figure 1C). This places them at the convergence of the open extracellular vestibule in a key fulcrum position for propagation of conformational rearrangements (Figure 1C, D, E). Residues involved in peptide-mediated bias faced principally towards the core of the bundle while the small polar serines implicated in global changes to signal bias exhibited a more peripheral localisation (Figure 1C, D).

Predicted interaction networks

In the revised model, R2.60^{190} is predicted to form H-bond interactions with E6.53^{364} and to a lesser extent N3.43^{240}. E6.53^{364} is also predicted to form H-bond interactions with both H6.52^{363} and Q7.49^{394}, suggesting that the central core network likely forms interdependent

Molecular Pharmacology Fast Forward. Published on December 23, 2015 as DOI: 10.1124/mol.115.101246
This article has not been copyedited and formatted. The final version may differ from this version.

interactions (Figure 1E); these interactions can also be seen in MD simulations (Supplemental Movie 1), and the stability of the interactions mapped from the MD trajectories (Supplemental Figure 1).

To gain further insight into the nature of these interactions and their role in controlling peptide-dependent signaling, we generated an additional series of mutations that comprised E6.53^{364}A, N3.43^{240}Q, Q7.49^{394}N and the double mutant N3.43^{240}Q/ Q7.49^{394}N. These mutants were designed to test the importance of the interaction between E6.53^{364} and R2.60^{190}, and the hydrogen bonding patterns arising from N3.43^{240} and Q7.49^{394}. The mutants were analysed for effect on peptide binding and receptor activation of canonical signaling pathways (cAMP accumulation, pERK1/2 and iCa^{2+} mobilisation). Functional data were analysed using the operational model (Black & Leff, 1983), to calculate effects on efficacy independent of those on affinity. Quantitative data was also generated for the N3.43^{240}A/ Q7.49^{394}A double mutant that was qualitatively reported previously (Wootten et al., 2013a).

Effect of mutation on receptor expression and agonist peptide binding

Consistent with the previous observation of decreased cell surface expression and affinity for GLP-1, exendin-4 and exendin(9-39) for R2.60^{190}A (Wootten et al., 2013a), the E6.53^{364}A mutant also decreased cell surface expression and the affinity of these peptides, but not that of oxyntomodulin (Figure 2, Table 2). Cell surface receptor expression was not significantly affected by Q7.49^{394}N, and only a small decrease (~20%) in Bmax was seen with the N3.43^{240}Q or N3.43^{240}Q/ Q7.49^{394}N mutants (Figure 2E, F). Oxyntomodulin affinity was not altered by any of these mutants (Figure 2C, Table 2). Neither the Q7.49^{394}N nor the N3.43^{240}Q mutants significantly altered affinity for any of the peptides while the N3.43^{240}Q/

Molecular Pharmacology Fast Forward. Published on December 23, 2015 as DOI: 10.1124/mol.115.101246
This article has not been copyedited and formatted. The final version may differ from this version.

Q7.49^{394}N double mutant significantly decreased exendin-4 and exendin(9-39) affinity, but not that of GLP-1 (Figure 2A-D, Table 2).

Effect of mutation on cAMP production

Only the E6.53^{364}A mutant significantly attenuated cAMP signaling by exendin-4 and this is consistent with the loss of signaling seen previously with the R2.60^{190} mutant (Figure 3E, H, Table 3).

The E6.53^{364}A mutation also reduced GLP-1 efficacy, but this peptide was more broadly affected by mutation of other amino acids in the network (Figure 3A, D, G, Table 3). As previously reported N3.43^{240}A significantly attenuated signaling (Wootten et al., 2013), while the N3.43^{240}A/ Q7.49^{394}A double mutant yielded a similar level of impairment (Figure 2A, D). Interestingly, the N3.43^{240}Q mutant had very little effect. Likewise, there was no significant loss of signaling with the N3.43^{240}Q/ Q7.49^{394}N double mutant (Figure 3A, D).

While mutational analysis provides increasing evidence for differences in the mechanism of receptor activation by GLP-1 and exendin-4, oxyntomodulin exhibits biased signaling for canonical pathways even at the wild-type receptor (Koole et al., 2010; Willard et al., 2013), and this is reflected in the effect of mutations on oxyntomodulin-mediated signaling. In contrast to GLP-1 and exendin-4, neither the E6.53^{364}A nor the R2.60^{190}A (Wootten et al., 2013) mutant impaired oxyntomodulin-mediated cAMP formation (Figure 3C, F, I, Table 3); indeed the R2.60^{190}A mutant augmented signaling. Interestingly, the most critical residues in this network were Q7.49^{394} and H6.52^{363}. Both the Q7.49^{394}N and the previously published

Molecular Pharmacology Fast Forward. Published on December 23, 2015 as DOI: 10.1124/mol.115.101246
This article has not been copyedited and formatted. The final version may differ from this version.

Q7.49^{394}A attenuated signaling. Also of note, the N3.43^{240}Q/ Q7.49^{394}N mutant was more detrimental than the N3.43^{240}A/ Q7.49^{394}A mutant.

H6.52^{363} is critical for cAMP production by all three peptides (Wootten et al., 2013a, Figure 3, Table 3), and this may be a common component of all signaling to this pathway, albeit that the mechanism driving changes to the residue may be different for individual peptides.

Effect of mutation on calcium mobilisation

The network required for calcium mobilisation was distinct from that for cAMP generation for each of the peptides. For both GLP-1 (Figure 4A, D, G) and exendin-4 (Figure 4B, E, H), Q7.49^{394} and H6.52^{363} are critical for this signaling (Wootten et al., 2013a; Table 3). R2.60^{190} and E6.53^{364} were not required, as mutation to alanine did not significantly alter efficacy (Figure 4D, E, Table 3), thus, unlike cAMP signaling the predicted interaction between these residues is not required for iCa^{2+} mobilisation. In addition, for both GLP-1 and exendin-4, N3.43^{240} also appeared to play a limited role in efficacy. For exendin-4, the N3.43^{240}A mutation was detrimental (Wootten et al., 2013a; Figure 4E, Table 3), while the N3.43^{240}Q displayed significantly different efficacy in response to GLP-1 (Figure 4D, Table 3), nonetheless a similar trend to decrease efficacy was observed for the non-significant mutations of this amino acid for the two peptides. Interestingly, for oxyntomodulin, although Q7.49^{394} was also critical for calcium signaling (Figure 4C, F, I, Table 3), H6.52^{363} was not required. Instead, both R2.60^{190}A and E6.53^{364}A enhanced signaling, although this latter effect did not reach significance (Figure 4F, Table 3; Wootten et al., 2013a). In the wild-type receptor, R2.60^{190} and E6.53^{364} may retard the efficiency of oxyntomodulin-mediated signaling by limiting the conformational sampling available to Q7.49^{394} (Figure 4I). Although

Molecular Pharmacology Fast Forward. Published on December 23, 2015 as DOI: 10.1124/mol.115.101246
This article has not been copyedited and formatted. The final version may differ from this version.

the N3.43^{240}A mutation did not have a significant effect on oxyntomodulin signaling, N3.43^{240}Q caused marked attenuation of signaling (Figure 4F, Table 3).

Effect of mutation on ERK1/2 phosphorylation

The pattern of effect of mutation on peptide-mediated pERK1/2 was similar for GLP-1 (Figure 5A, D, G) and exendin-4 (Figure 5B, E, H), although subtle differences were observed. Both R2.60^{190} and E6.53^{364} appeared to be important, albeit that the E6.53^{364}A mutant effect did not reach significance for GLP-1 (Figure 5D, E, Table 3; Wootten et al., 2013a). Neither N3.43^{240}Q, Q7.49^{394}N, nor the N3.43^{240}Q/ Q7.49^{394}N double mutant had any effect on efficacy, however, as described previously (Wootten et al., 2013), N3.43^{240}A either increased efficacy (exendin-4) or had no effect (GLP-1), and the Q7.49^{394}A mutant decreased efficacy mediated by GLP-1 but this effect was not significant for exendin-4, although it followed the same trend (Figure 5D, E, Table 3; Wootten et al., 2013a). In both cases, the N3.43^{240}A/ Q7.49^{394}A mutant was detrimental, while H6.52^{363}A was the most unfavourable of the mutations in this network (Figure 5D, E, Table 3). In contrast, oxyntomodulin was minimally affected by any of the mutations; a limited decrease in efficacy with the N3.43^{240}Q/ Q7.49^{394}N double mutant being the only significant effect (Figure 5C, F, I, Table 3).

Molecular Pharmacology Fast Forward. Published on December 23, 2015 as DOI: 10.1124/mol.115.101246
This article has not been copyedited and formatted. The final version may differ from this version.

Discussion

Class B peptide hormone receptors are critical for normal physiology and are significant targets for potential treatment of major disease, including diabetes and obesity. As such, understanding how peptides interact with and activate these receptors is fundamentally important. The recent solution of structures of the transmembrane domain of the glucagon and CRF1 receptors has provided novel insight into the nature of the core region of the receptor that is responsible for the allosteric transition that occurs upon peptide binding to enable effector coupling. In the inactive state, these receptors present a very open extracellular face that is likely to be hydrated (Siu et al., 2013; Hollenstein et al., 2013, Hollenstein et al., 2014), suggesting that a key component of the binding and activation process may involve bulk displacement of water and/or the reordering of hydrogen bond networks; the latter is consistent with the current understanding of receptor activation for class A receptors (Illergard et al., 2011; Zhou et al., 2000; Curran et al., 2003; Angel et al., 2009).

We previously reported the identification of a key network of amino acids in the GLP-1 receptor comprising R2.60^{190}, N3.43^{240} and Q7.49^{394} that, when mutated, differentially altered the signaling of the peptide agonists, GLP-1, exendin-4 and oxyntomodulin (Wootten et al., 2013a). In the current study we have used the recent structural information on class B GPCRs to re-evaluate our understanding of this network. Key differences in the original and revised GLP-1 receptor models included the relative positioning of E6.53^{364} and H6.52^{363}, within this network, and N5.50^{320} that, although important for signaling, was not predicted to directly interact with the network in the revised model. Interestingly, this led to clustering of key residues in a fulcrum position at the convergence of the extracellular ends of the TM helices (Figure 1C, D). The nature of the revised interaction network thus formed was further explored via mutation of E6.53^{364} that is predicted to interact with R2.60^{190}, along with

Molecular Pharmacology Fast Forward. Published on December 23, 2015 as DOI: 10.1124/mol.115.101246
This article has not been copyedited and formatted. The final version may differ from this version.

conservative changes to N3.43[240] and Q7.49[39], extending or reducing the side chain length, respectively in a manner that probed likely importance of hydrogen bonding.

Comparison of the equivalent amino acid side chains in the glucagon and CRF1 structures revealed conservation in relative orientation of side chains (Figure 6A-C), even though quite distinct residues occurred in TM6 of the CRF1 receptor, namely Tyr at 6.53 and Thr at 6.52. In the glucagon receptor, maintenance of this network may be partially coordinated by water-mediated H-bonding (Figure 6D). Thus this network is likely to be highly constrained in the inactive state of the receptor. Indeed, in the glucagon receptor, the position of K2.60 (equivalent to R2.60 in the GLP-1 and CRF1 receptors) is restricted by H-bonding to S7.46 that in turn interacts with Y1.47, suggesting that one component of activation may include release of these constraints on amino acid 2.60, allowing reordering of the network. In the GLP-1 receptor homology model, a similar interaction between T7.46[391] and R2.60[190]/E6.53[364] is predicted to occur (Figure 7A). Nonetheless, T7.46[391]A had limited effect on GLP-1 affinity and cAMP formation (Coopman et al., 2011), suggesting that other interactions predominate, at least for activation of this pathway. In the current study, we have modelled a GLP-1 bound form of the full-length receptor that incorporates known distance constraints from published cross-linking studies (Figure 7B), and this model is generally consistent with that for the modelled peptide-bound glucagon receptor where the peptide forms an extended helix and the N-terminus of the peptide binds within the open cavity of the TM bundle (Siu et al., 2013; Yang et al., 2015). In our model, the GLP-1 peptide is predicted to bind deep within the TM bundle and is associated with disruption of the central H-bond network (Figure 7A versus Figure 7B).

Molecular Pharmacology Fast Forward. Published on December 23, 2015 as DOI: 10.1124/mol.115.101246
This article has not been copyedited and formatted. The final version may differ from this version.

As previously noted, the GLP-1 receptor exhibits peptide-dependent biased agonism across the canonical signaling pathways of cAMP formation, calcium mobilisation and ERK phosphorylation and this is most notable for oxyntomodulin, which is biased towards pERK1/2 at the wild-type receptor (Koole et al., 2010; Wootten et al., 2013b; Willard et al., 2013). While GLP-1 and exendin-4 have similar bias for these pathways at the wild-type receptor there is increasing evidence from mutational studies that these peptides have distinct modes of receptor activation (Koole et al., 2012, Wootten et al., 2013a), and this is also supported by differences in peptide-mediated activation of G protein chimeras in yeast (Weston et al., 2014). The current study provides additional evidence for how these peptides use the central polar network to drive activation of the receptor. The use of operational, analytical modelling of functional responses enables the separation of mutational effects on affinity from those on efficacy and allows the impact of mutation on different signaling endpoints to be measured.

Potential mechanisms driving pathway specific signaling

For GLP-1 and exendin-4, the principal driver for cAMP generation is the interaction between R2.60^{190} and E6.53^{364} that likely leads to conformational rearrangement of TM6. It is possible that this is initiated by release of H-bond interactions with upstream polar residues that are observed in the inactive glucagon receptor. In the case of GLP-1, optimal efficiency for this interaction is predicted to involve coordination of the position of R2.60^{190} through hydrogen bonding with N3.43^{240} that may favour interaction with peptide side-chain residues, in particular between R2.60^{190} and Glu at residue 3 (amino acid 9, where His^{7} is the first residue of GLP-1(7-36)NH_2) of the GLP-1 (Figure 7B) and exendin-4 peptides. This constraint can also be maintained by Gln substitution of 3.43, potentially by allowing more efficient

Molecular Pharmacology Fast Forward. Published on December 23, 2015 as DOI: 10.1124/mol.115.101246
This article has not been copyedited and formatted. The final version may differ from this version.

hydrogen bonding to occur. In contrast, oxyntomodulin-mediated cAMP formation is driven via Q7.49^{394} and H6.52^{363}, and could potentially involve formation of a hydrogen bond between these two amino acids, when the interaction between R2.60^{190} and E6.53^{364} is not fully disrupted (Figure 3I). H6.52^{363} is a critical residue for all peptide-mediated cAMP formation through rearrangement of the side chain on activation, speculatively through either loss of interaction with E6.53^{364}, via either disruption of the E6.53^{364}/R2.60^{190} interaction (GLP-1, exendin-4), or via formation of a novel interaction with Q7.49^{394} (oxyntomodulin).

In contrast to the requirements for cAMP formation, peptide-mediated calcium mobilisation does not require alteration to the interaction between R2.60^{190} and E6.53^{364} (Figure 4G-I). The common, critical residue for calcium mobilisation by all peptides is Q7.49^{394}. For GLP-1 and exendin-4, H6.52^{363} is also critical. This amino acid potentially forms interactions with Q7.49^{394} that constrains conformational sampling required for efficacy. The selective effects of other mutations may support importance of conformational flexibility of Q7.49^{394} for calcium signaling, albeit in a peptide-selective manner. E6.53^{364} is predicted to H-bond directly with Q7.49^{394}, constraining its mobility. For oxyntomodulin, which does not appear to activate the receptor in a manner that modifies interactions of R2.60^{190}, the H-bond interaction between R2.60^{190} and E6.53^{364} potentially constrains the interaction between E6.53^{364} and Q7.49^{394} leading to reduced efficiency of signaling such that R2.60^{190}A mutation increases efficacy. As noted for cAMP, subtle differences in mechanism of receptor activation also occur for GLP-1 and exendin-4 and this is also seen for calcium signaling where the magnitude of effect for mutation of N3.43^{240} to Ala or Gln differs for the two peptides. We speculate that N3.43^{240} can also interact with R2.60^{190} and that this may in turn alter interactions with Q7.49^{394} indirectly via events coordinated through E6.53^{364} (Figure 4G, H).

Molecular Pharmacology Fast Forward. Published on December 23, 2015 as DOI: 10.1124/mol.115.101246
This article has not been copyedited and formatted. The final version may differ from this version.

While cAMP production and calcium mobilisation are predominately G protein mediated, the transient phosphorylation of ERK1/2 is the result of convergent signaling of both G protein-dependent and independent effectors (Montrose-Rafizadeh et al., 1999; Baggio and Drucker, 2006). As seen with cAMP accumulation, the interaction between R2.60^{190} and E6.53^{364} (Figure 5G, H) appeared to be required for efficient GLP-1 and exendin-4 mediated pERK1/2, albeit that the magnitude of effect tended to be greater for the cAMP response. Likewise, H6.52^{363} was also critical for the response of these peptides, and this may be indicative of a significant contribution of G proteins to ERK1/2 signaling. N3.43^{240} and Q7.49^{394} played distinct roles for GLP-1 and exendin-4, but only in the context of non-conservative mutation and may imply a differential role of these residues in coordination with R2.60^{190} and/or E6.53^{364} for the two peptides.

In contrast to the effect of mutation on GLP-1 and exendin-4 mediated pERK1/2, there was very little effect of any of the mutants on oxyntomodulin-mediated signaling (Figure 2J), with only the N3.43^{240}Q/Q7.49^{394}N double mutant significantly attenuating the response. This is consistent with the strong bias seen with oxyntomodulin for pERK1/2 versus cAMP or iCa^{2+} signaling (Koole et al., 2010; Willard et al., 2013; Wootten et al., 2013b). It may also imply distinction in the extent of engagement with different effectors. Thus the central network exemplified in the current study may be critical for G protein-mediated signaling but play a lesser role in non-G protein-dependent signaling. Furthermore, in addition to emphasising major differences in receptor activation by oxyntomodulin compared to GLP-1 and exendin-4, the current work provides additional evidence of differences in the mechanism of activation transition elicited by GLP-1 and exendin-4. Recent work using chimeric G proteins in yeast indicates that exendin-4, as well as oxyntomodulin, may be biased towards Gi over Gs when

Molecular Pharmacology Fast Forward. Published on December 23, 2015 as DOI: 10.1124/mol.115.101246
This article has not been copyedited and formatted. The final version may differ from this version.

compared to GLP-1 (Weston et al., 2014), while arrestin recruitment studies also support distinct bias between GLP-1 and exendin-4 (Wootten et al., 2013b).

The conservation of key residues in the network and its fulcrum position in the structure of class B GPCRs suggests that it is likely to play a critical role in signaling for this subfamily. However, the distinctions in the data for different ligands of the GLP-1 receptor indicate that the specific mechanism of receptor activation is likely to be different for individual receptor ligand combinations. There is supporting data from studies of other class B receptors of the critical role of this network in receptor activation, with interaction of R2.60^{188}, N3.43^{229} and Q7.49^{380} predicted from mutagenesis and modelling studies of the VPAC1 receptor (Chugunov et al., 2010; Langer, 2012; Solano et al., 2001). Intriguingly, R2.60^{188} is predicted to interact via a salt-bridge with D^{3} of vasoactive intestinal peptide, with this interaction contributing to receptor activation (Langer, 2012); the equivalent amino acid in GLP-1 and exendin-4 is Glu, while it is a Gln in oxyntomodulin. Modelling of GLP-1 peptide docking to the full-length receptor is consistent with formation of a direct, salt-bridge, interaction between peptide Glu^{9} and R2.60^{190} (Figure 7B). It is interesting to speculate that lack of an acidic residue at the third amino acid of oxyntomodulin may underlie the lack of engagement of the R2.60^{190}/E6.53^{364} interaction in receptor activation.

Collectively, this work expands our understanding of peptide-mediated signaling from the GLP-1 receptor and the key role that the central polar network plays in these events. The ever-increasing availability of high-resolution structural data provides better understanding of the atomic events that are likely to drive receptor activation, though the dynamic nature of activation transition and the distinct ability of individual ligands to affect this process means

Molecular Pharmacology Fast Forward. Published on December 23, 2015 as DOI: 10.1124/mol.115.101246
This article has not been copyedited and formatted. The final version may differ from this version.

that we will still require multiple approaches to derive an accurate understanding of these dynamics.

Molecular Pharmacology Fast Forward. Published on December 23, 2015 as DOI: 10.1124/mol.115.101246
This article has not been copyedited and formatted. The final version may differ from this version.

Author contributions

Participated in research design: Wootten, Sexton

Conducted experiments: Wootten, Reynolds, Smith, Mobarec, Quon, Simms, Coudrat

Contributed new reagents or analytic tools: N/A

Performed data analysis: Wootten, Koole, Mobarec, Sexton, Christopoulos

Wrote or contributed to the writing of the manuscript: Wootten, Koole, Reynolds, Furness, Miller, Christopoulos, Sexton

References

Angel TE, Chance MR, Palczewski K (2009). Conserved waters mediate structural and functional activation of family A (rhodopsin-like) G protein-coupled receptors. *Proc Natl Acad Sci USA* **106:**8555–8560.

Baggio LL, and Drucker DJ (2006). Therapeutic approaches to preserve islet mass in type 2 diabetes. *Annu Rev Med* **57:**265-281.

Baggio LL, and Drucker DJ (2007). Biology of incretins: GLP-1 and GIP. *Gastroenterology.* **132:**2131-2157.

Black JW, and Leff P (1983). Operational models of pharmacological agonism. *Proc R Soc Lond B Biol Sci* **220:**141-162.

Caltabiano G, Gonzalez A, Cordomí A, Campillo M, Pardo L (2013). The role of hydrophobic amino acids in the structure and function of the rhodopsin family of G protein-coupled receptors. *Methods Enzymol.* **520:**99-115.

Chen Q, Pinon DI, Miller LJ, and Dong MQ (2009). Molecular basis of glucagon-like peptide 1 docking to its intact receptor studied with carboxyl-terminal photolabile probes. *J Biol Chem* **284:**34135-34144.

Chen Q, Pinon DI, Miller LJ, Dong M (2010). Spatial approximations between residues 6 and 12 in the amino-terminal region of glucagon-like peptide 1 and its receptor: a region critical for biological activity. *J Biol Chem* **285:**24508-24518.

Cheong YH, Kim MK, Son MH, Kaang BK (2012). Two small molecule agonists of glucagon-like peptide-1 receptor modulate the receptor activation response differently. *Biochem Biophys Res Commun*. **417:**558-563.

Chugunov AO, Simms J, Poyner DR, Dehouck Y, Rooman M, Gilis D, and Langer I (2010). Evidence that interaction between conserved residues in transmembrane helices 2, 3, and 7 are crucial for human VPAC1 receptor activation. *Mol Pharmacol* **78:**394-401.

Coopman K, Huang Y, Johnston N, Bradley SJ, Wilkinson GF, Willars GB (2010). Comparative effects of the endogenous agonist glucagon-like peptide-1 (GLP-1)-(7-36) amide and the small-molecule ago-allosteric agent "compound 2" at the GLP-1 receptor. *J Pharmacol Exp Ther* **334:**795-808.

Coopman K, Wallis R, Robb G, Brown AJH, Wilkinson GF, Timms, and Willars GB (2011). Residues within the transmembrane domain of the glucagon-like peptide-1 receptor involved in ligand binding and receptor activation: modelling of the ligand-bound receptor. *Mol Endocrinol* **25:**1804-1818.

Curran AR, Engelman DM (2003). Sequence motifs, polar interactions and conformational changes in helical membrane proteins. *Curr Opin Struct Biol* **13:**412–417.

Eswar N, Webb B, Marti-Renom MS, Madhusudham DE, Shen MY, Pieper U, and Sali A (2007). Comparative protein structure modeling with MODELLER. *Curr Protocols Bioinform* 2.9.1-2.9.31.

Friesner RA, Banks JL, Murphy RB, Halgren TA, Klicic JJ, Mainz DT, Repasky MP, Knoll EH, Shelley M, Perry JK, Shaw DE, Francis P, and Shenkin PS (2004). Glide: A new approach for rapid, accurate docking and scoring. 1. Method and assessment of docking accuracy. *J Med Chem* **47:**1739-1749.

Harvey MJ, Giupponi G, and De Fabritiis G (2009) ACEMD: Accelerating biomolecular dynamics in the microsecond time scale. *J Chem Theory Comp* **5:** 1632-1639.

Hoang HN, Song K, Hill TA, Derksen DR, Edmonds DJ, Kok WM, Limberakis C, Liras S, Loria PM, Mascitti V, Mathiowetz AM, Mitchell JM, Piotrowski DW, Price DA, Stanton RV, Suen JY, Withka JM, Griffit DA, and Fairlie DP (2015). Short hydrophobic peptides with cyclic constraints are potent glucagon-like peptide-1 receptor (GLP-1R) agonists. *J Med Chem* **58:**4080-4085.

Hollenstein K, Kean J, Bortolato A, Cheng RK, Dore AS, Jazayeri A, Cooke RM, Weir M, and Marshall FH (2013). Structure of class B GPCR corticotropin-releasing factor receptor 1. *Nature* **499:**438-443.

Hollenstein K, de Graaf C, Bortolato A, Wang MW, Marshall FH, Stevens RC (2014). Insights into the structure of class B GPCRs. *Trends Pharmacol Sci.* **35:**12-22.

Hornak V, Abel R, Okur A, Strockbine B, Roitberg A, and Simmerling C (2006) Comparison of multiple Amber force fields and development of improved protein backbone parameters. *Proteins* **65:** 712-725.

Illergård K, Kauko A, Elofsson A (2011). Why are polar residues within the membrane core evolutionary conserved? *Proteins* **79:**79–91.

Jacobson MP, Pincus DL, Rapp CS, Day TJ, Honig B, Shaw DE, and Friesner RA (2004). A hierarchical approach to all-atom protein loop prediction. *Proteins* **55:**351-367.

Jorgensen R, Kubale V, Vrecl M, Schwartz TW, Elling CE (2007). Oxyntomodulin differentially affects glucagon–like peptide–1 receptor β-arrestin recruitment and signaling through Gα(s*). J Pharmacol Exp Ther* **322:**148–154.

Katritch V, Fenalti G, Abola EE, Roth BL, Cherezov V, Stevens RC (2014). Allosteric sodium in class A GPCR signaling. *Trends Biochem Sci*. **39:**233-244.

Kenakin T, Christopoulos A (2013). Signalling bias in new drug discovery: detection, quantification and therapeutic impact. *Nat Rev Drug Discov* **12:**205-216.

Kenakin T, Watson C, Muniz-Medina V, Christopoulos A, Novick S (2012). A simple method for quantifying functional selectivity and agonist bias. *ACS Chem Neurosci* **3:**193-203.

Koole C, Wootten D, Simms J, Valant C, Sridhar R, Woodman OL, Miller LJ, Summers RJ, Christopoulos A, and Sexton PM (2010). Allosteric ligands of the glucagon-like peptide 1 receptor (GLP-1R) differentially modulate endogenous and exogenous peptide responses in a pathway-selective manner: Implications for drug screening. *Mol Pharmacol* **78:**456-465.

Koole C, Wootten D, Simms J, Valant C, Miller LJ, Christopoulos A, and Sexton PM (2011). Polymorphism and Ligand Dependent Changes in Human Glucagon-Like Peptide-1 Receptor (GLP-1R) Function: Allosteric Rescue of Loss of Function Mutation. *Mol Pharmacol* **80:**486-497.

Koole C, Wootten D, Simms J, Miller LJ, Christopoulos A, and Sexton PM (2012a). Second Extracellular Loop of Human Glucagon-like Peptide-1 Receptor (GLP-1R) Has a Critical Role in GLP-1 Peptide Binding and Receptor Activation. *J Biol Chem* **287:**3642-3658.

Koole C, Wootten D, Simms J, Savage EE, Miller LJ, Christopoulos A, and Sexton PM (2012b). Second Extracellular Loop of Human Glucagon-like Peptide-1 Receptor (GLP-1R) Differentially Regulates Orthosteric but Not Allosteric Agonist Binding and Function. *J Biol Chem* **287:**3659-3673.

Koole C, Pabreja K, Savage EE, Wootten D, Furness SG, Miller LJ, Christopoulos A, and Sexton PM (2013). Recent advances in understanding GLP-1R (glucagon-like peptide-1 receptor) function. *Biochem Soc Trans* **41:**172-179.

Langer I (2012). Conformational switches in the VPAC(1) receptor. *Br J Pharmacol* **166:**79-84.

May LT, Avlani VA, Langmead CJ, Herdon HJ, Wood MD, Sexton PM, and Christopoulos A (2007). Structure-function studies of allosteric agonism at M2 muscarinic acetylcholine receptors. *Mol Pharmacol* **72:**463-476.

Miller LJ, Chen Q, Lam PC, Pinon DI, Sexton PM, Abagyan R, Dong M (2011). Refinement of glucagon-like peptide 1 docking to its intact receptor using mid-region photolabile probes and molecular modeling. *J Biol Chem* **286:**15895-15907.

Montrose-Rafizadeh C, Avdonin P, Garant MJ, Rodgers BD, Kole S, Yang H, Levine MA, Schwindinger W, Bernier M (1999). Pancreatic glucagon-like peptide-1 receptor couples to multiple G proteins and activates mitogen-activated protein kinase pathways in Chinese hamster ovary cells. *Endocrinology* **140:**1132-1140.

Moon MJ, Lee YN, Park S, Reyes-Alcaraz A, Hwang JI, Millar RP,Choe H, and Seong JY (2015). Ligand binding pocket formed by evolutionarily conserved residues in the glucagon-like peptide-1 (GLP-1) receptor core domain. *J Biol Chem* **290:**5696-5706.

Pabreja ., Mohd MA, Koole C, Wootten D, and Furness SGB (2014) Molecular mechanisms underlying physiological and receptor pleiotropic effects mediated by GLP-1R activation. *Brit J Pharmacol* **171:** 1114–1128.

Rasmussen SGF, DeVree BT, Zou YZ, Kruse AC, Chung KY, Kobilka TS, Thian FS, Chae PS, Pardon E, Calinski D, Mathiesen JM, Shah STA, Lyons JA, Caffrey M, Gellman SH, Steyaert J, Skiniotis G, Weis WI, Sunahara RK, Kobilka BK (2011). Crystal structure of the beta(2) adrenergic receptor-Gs protein complex. *Nature* **477:**549-555.

Shonberg J, Lopez L, Scammells PJ, Christopoulos A, Capuano B, Lane JR (2014). Biased agonism at G protein-coupled receptors: the promise and the challenges--a medicinal chemistry perspective. *Med Res Rev.* **34:**1286-1330.

Siu FY, He M, de Graaf C, Han GW, Yang D, Zhang Z, Zhou C, Xu Q, Wacker D, Joseph JS, Liu W, Lau J, Cherezov V, Katritch V, Wang MW, and Stevens RC (2013). Structure of the human glucagon class B G-protein-coupled receptor. *Nature* **499:**444-449.

Solano RM, Langer I, Perret J, Vertongen P, Juarranz MG, Robberecht P, and Waelbroeck M (2001). Two basic residues of the h-VPAC1 receptor second transmembrane helix are essential for ligand binding and signal transduction. *J Biol Chem* **276:**1084-1088.

Taddese B, Upton GJ, Bailey GR, Jordan SR, Abdulla NY, Reeves PJ, Reynolds CA (2014). Do plants contain G protein-coupled receptors? *Plant Physiol* **164:**287-307.

Tubert-Brohman I, Sherman W, Repasky M, and Beuming T (2013). Improved docking of polypeptides with Glide. *J Chem Inf Model* **53:**1689-1699.

Underwood CR, Garibay P, Knudsen LB, Hastrup S, Peters GH, Rudolph R, and Reedtz-Runge S (2010). Crystal structure of glucagon-like peptide-1 in complex with the extracellular domain of the glucagon-like peptide-1 receptor. *J Biol Chem* **285:**723-730.

Venkatakrishnan AJ, Deupi X, Lebon G, Tate CG, Schertler GF, Babu MM (2013). Molecular signatures of G-protein-coupled receptors. *Nature.* **494:**185-194.

Vertongen P, Solano RM, Perret J, Langer I, Robberecht P, and Waelbroeck M (2001). Mutational analysis of the human vasoactive intestinal peptide receptor subtype VPAC(2):

role of basic residues in the second transmembrane helix. *British J Pharmacol* **133:**1249-1254.

24. Walker RC, Dickson CJ, Madej BD, Skjevik AA, Betz RM, Teigen K, and Gould IR (2014) Amber lipid force field: Lipid14 and beyond. *Abstracts of Papers of the American Chemical Society* **2014,** 248.

Weston C, Poyner D, Patel V, Dowell S, and Ladds G (2014). Investigating G protein signaling bias at the glucagon-like peptide-1 receptor in yeast. *Br J Pharmacol* **171:**3651-3665.

Willard FS, Wootten D, Showalter AD, Savage EE, Ficorilli J, Farb TB, Bokvist K, Alsina-Fernandez J, Furness SG, Christopoulos A, Sexton P, and Sloop KW (2012). Small molecule allosteric modulation of the glucagon-like peptide-1 receptor enhances the insulinotropic effect of oxyntomodulin. *Mol Pharmacol* **82:** 1066-1073.

Wootten D, Simms J, Miller LJ, Christopoulos A, and Sexton PM (2013a). Polar transmembrane interactions drive formation of ligand-specific and signal pathway-biased family B G protein-coupled receptor conformations. *Proc Natl Acad Sci U S A* **110:**5211-5216.

Wootten D, Savage EE, Willard FS, Bueno AB, Sloop KW, Christopoulos A, and Sexton PM (2013b). Differential activation and modulation of the glucagon-like peptide-1 receptor by small molecule ligands. *Mol Pharmacol* **83:**822-834.

Yang L, Yang D, de Graaf C, Moeller A, West GM, Dharmarajan V, Wang C, Siu FY, Song G, Reedtz-Runge S, Pascal BD, Wu B, Potter CS, Zhou H, Griffin PR, Carragher B, Yang H, Wang MW, Stevens RC, and Jiang H (2015). Conformational states of the full-length glucagon receptor. *Nat Commun* **6:**7859. doi: 10.1038/ncomms8859.

Zhou FX, Cocco MJ, Russ WP, Brunger AT, Engelman DM (2000). Interhelical hydrogen bonding drives strong interactions in membrane proteins. *Nat Struct Biol* **7:**154–160.

Footnotes

This work was supported by National Health and Medical Research Council of Australia (NHMRC) project grants [1061044] and [1065410], and NHMRC program grant [1055134]; Biotechnology and Biological Sciences Research Council of the United Kingdom project grant [BB/M006883/1], and Medical Research Council (UK) grant [G1001812]. PMS and AC are NHMRC Principal Research Fellows. DW is a NHMRC Career Development Fellow. CK is a NHMRC CJ Martin Postdoctoral Fellow. TC is the recipient of a Victorian Life Sciences Computing Initiative (VLSCI) scholarship. The computational studies were supported by resource allocation scheme grant no. VR0024 of the Victorian Life Sciences Computation Initiative (VLSCI) on its Peak Computing Facility at the University of Melbourne. The current address for Cassandra Koole is: Laboratory of Chemical Biology & Signal Transduction, The Rockefeller University, New York, NY 10065, U.S.A.

Molecular Pharmacology Fast Forward. Published on December 23, 2015 as DOI: 10.1124/mol.115.101246
This article has not been copyedited and formatted. The final version may differ from this version.

Figure Legends

Figure 1. *Comparison of original **A** (Wootten et al., 2013a) and new apo homology model of the human GLP-1 receptor **B-E***. R2.60^{190}, N3.43^{240}, H6.52^{363}, E6.53^{364}, and Q7.49^{394} comprise key residues involved in peptide-mediated signaling bias. **A.** and **B.** depict top down views of the transmembrane bundle and positioning of key amino acids (as x-stick, coloured by amino acid side chain). The major differences include opening of the extracellular vestibule, clockwise rotation of TM6 and intracellular offset of TM5 by 2 helical turns. **C.** and **D.** Homology model illustrating the relative position of R2.60^{190}, N3.43^{240}, H6.52^{363}, E6.53^{364}, and Q7.49^{394}, residues involved in peptide-mediated signaling bias, depicted with red space fill, and S.150^{155}, S2.56^{186}, S7.47^{392}, blue space fill, small polar residues involved in intramembraneous packing and are globally involved in receptor-dependent signal bias. These residues sit in a fulcrum position at the convergence of the helices, with the residues involved in ligand-dependent signal bias located within the core of the receptor. **C.** view from the transmembrane face of the receptor. **D.** view from the extracellular space. **E.** The central polar network depicted as x-stick (coloured by amino acid side chain), illustrating predicted H-bonding within the network (coloured dotted lines; sphere size is proportional to predicted strength of interaction).

Figure 2. *Effect of mutation of the central polar network on peptide binding and cell surface receptor expression.* **A-D.** Inhibition of [^{125}I]-exendin(9-39) binding by agonist and antagonist peptides at the wild-type and new mutant receptors. For clarity, only data from new mutants, or previously not quantified, are displayed. **E.** Cell surface expression of mutant receptors (normalised to that of the wild-type receptor) as measured by anti-cmyc antibody binding to the N-terminal cmyc epitope in an ELISA. **F.** Cell surface expression of mutant receptors (normalised to that of the wild-type receptor) determined as Bmax from homologous

competition of [^{125}I]-exendin(9-39) binding by unlabeled exendin(9-39). Data are displayed as mean + S.EM. of four to seven independent experiments, conducted in duplicate. (*) Significantly different from wild-type receptor at P<0.05, ANOVA with Dunnett's post-test. V, vehicle. Data for expression of the previously published R2.60^{190}A, N3.43^{240}A, Q7.49^{394}A and H6.52^{363} receptor mutants (Wootten et al., 2013a) is included for comparison.

Figure 3. *Effect of mutation of the central polar network on peptide-mediated cAMP production.* Upper panels illustrate concentration-response curves for each of the peptides at the wild-type and mutant receptors with data fitted to the operational model. For clarity, only data from new mutants, or those previously not quantified, are displayed. Middle panels illustrate affinity-independent measures of efficacy (Log tau) determined by operational modeling of the data, corrected for receptor Bmax at the cell surface. **A.** GLP-1-mediated responses. **B.** exendin-4-mediated responses. **C.** oxyntomodulin-mediated responses. Data are displayed as mean ± S.EM. of four to six independent experiments, conducted in duplicate. (*) Significantly different from wild-type receptor at P<0.05, ANOVA with Dunnett's post-test. V, vehicle. Data for expression of the previously published R2.60^{190}A, N3.43^{240}A, Q7.49^{394}A and H6.52^{363} receptor mutants (Wootten et al., 2013a) is included for comparison. **G-I.** Molecular models (x-stick format) illustrating the predicted central interaction network and their impact on peptide-mediated cAMP formation. **G.** GLP-1; **H.** exendin-4; **I.** oxyntomodulin. Amino acids negatively impacted by mutation are coloured red, those positively impacted in green, while those unaffected are coloured by side-chain as in Figure 1E. Predicted H-bonds are displayed as dotted lines.

Figure 4. *Effect of mutation of the central polar network on peptide-mediated $_{i}Ca^{2+}$ mobilisation*. Upper panels illustrate concentration-response curves for each of the peptides at

Molecular Pharmacology Fast Forward. Published on December 23, 2015 as DOI: 10.1124/mol.115.101246
This article has not been copyedited and formatted. The final version may differ from this version.

the wild-type and mutant receptors with data fitted to the operational model. For clarity, only data from new mutants, or those previously not quantified, are displayed. Middle panels illustrate affinity-independent measures of efficacy (Log tau) determined by operational modeling of the data, corrected for receptor Bmax at the cell surface. **A.** GLP-1-mediated responses. **B.** exendin-4-mediated responses. **C.** oxyntomodulin-mediated responses. Data are displayed as mean ± S.EM. of four to six independent experiments, conducted in duplicate. (*) Significantly different from wild-type receptor at $P<0.05$, ANOVA with Dunnett's post-test. N.D., no response detected. V, vehicle. Data for expression of the previously published R2.60^{190}A, N3.43^{240}A, Q7.49^{394}A and H6.52^{363} receptor mutants (Wootten et al., 2013a) is included for comparison. **G-I.** Molecular models (x-stick format) illustrating the predicted central interaction network and their impact on peptide-mediated intracellular calcium mobilisation. **G.** GLP-1; **H.** exendin-4; **I.** oxyntomodulin. Amino acids negatively impacted by mutation are coloured red, those positively impacted in green, while those unaffected are coloured by side-chain as in Figure 1E. Predicted H-bonds are displayed as dotted lines.

Figure 5. *Effect of mutation of the central polar network on peptide-mediated ERK phosphorylation.* Upper panels illustrate concentration-response curves for each of the peptides at the wild-type and mutant receptors with data fitted to the operational model. For clarity, only data from new mutants, or those previously not quantified, are displayed. Middle panels illustrate affinity-independent measures of efficacy (Log tau) determined by operational modeling of the data, corrected for receptor Bmax at the cell surface. **A.** GLP-1-mediated responses. **B.** exendin-4-mediated responses. **C.** oxyntomodulin-mediated responses. Data are displayed as mean ± S.EM. of four to six independent experiments, conducted in duplicate. (*) Significantly different from wild-type receptor at $P<0.05$, ANOVA with Dunnett's post-test. V, vehicle. Data for expression of the previously published

Molecular Pharmacology Fast Forward. Published on December 23, 2015 as DOI: 10.1124/mol.115.101246
This article has not been copyedited and formatted. The final version may differ from this version.

R2.60^{190}A, N3.43^{240}A, Q7.49^{394}A and H6.52^{363} receptor mutants (Wootten et al., 2013a) is included for comparison. **G-I.** Molecular models (x-stick format) illustrating the predicted central interaction network and their impact on peptide-mediated ERK phosphorylation. **G.** GLP-1; **H.** exendin-4; **I.** oxyntomodulin. Amino acids negatively impacted by mutation are coloured red, those positively impacted in green, while those unaffected are coloured by side-chain as in Figure 1E. Predicted H-bonds are displayed as dotted lines.

Figure 6. Comparison of the central polar network in the inactive (inverse-agonist bound) structures of the glucagon receptor (x-stick with polar hydrogens displayed), **A, C, D,** and the inverse-agonist bound CRF1 receptor, **B, C**, illustrating that, despite divergence in amino acid sequence, the positionally equivalent residues have a similar orientation. **D.** Hydration of the glucagon receptor structure predicts potential water-mediated H-bond interactions within the network. Waters are illustrated in CPK format, red=oxygen, off-white=hydrogen.

Figure 7. *Human GLP-1 receptor homology models.* **A.** Apo, transmembrane domain, model (blue backbone), with middle and bottom (180 degree rotation from the middle panel) panels illustrating the central polar interaction network (x-stick, coloured by amino acid side chain) and predicted H-bond interactions (coloured dotted lines). **B.** Full-length receptor model (orange backbone), bound to GLP-1(7-36)NH_2 (pink) and C-terminal G protein peptide (red); middle and bottom (180 degree rotation from the middle panel) panels illustrate the central polar interaction network (x-stick, coloured by amino acid side chain) and predicted disruption of the inactive network interactions. In this model, a direct interaction between peptide E^{9} and receptor R2.60^{190} is predicted to occur.

Table 1. ***Major constraints used in Modeller.***

GLP-1R position (A)	GLP-1 position (B)	Origin for GLP-1R – GLP-1 constraint	Constraint[a] (Å)	Reference
ECD; E133; C_γ	A24; C_β	Bpa^{24} GLP-1 photoaffinity crosslink.	$r_{AB} \leq 9.0$	Chen *et al.,* 2009[c]
TM1; L141;$C_{\delta1}$	V16; $C_{\gamma1}$	Bpa^{16} GLP-1 photoaffinity crosslink.	$r_{AB} \leq 9.0$	Miller *et al.*, 2011
TM1; Y145;C_ξ	F12; C_γ	Bpa^{12} GLP-1 photoaffinity crosslink.	$r_{AB} \leq 6.0$	Chen *et al.*, 2010
ECL2; W297;$C_{\eta2}$	L20; C_γ	Bpa^{20} GLP-1 photoaffinity crosslink.	$r_{AB} \leq 9.0$	Miller *et al.*, 2011
TM2; K197;N_ξ	E9; $O_{\varepsilon2}$	Reciprocal mutagenesis of residues between VIP and VIP-R-1/VIP-R-2 resulting in gain of function[b]	$r_{AB} \leq 4.0$	Solano et al., 2001;Vertongen et al., 2001
ECL3; R380;$N_{\eta2}$	D15; $O_{\varepsilon2}$	Reciprocal mutagenesis of residues between GLP-1 and GLP-1R resulting in gain of function.	$r_{AB} \leq 4.0$	Moon *et al.*, 2015

a These distances constraints were estimated from preliminary models that used tyrosine to represent BPA since the O_η of the tyrosine is topologically equivalent to the reactive carbon atom of BPA; A 6 Å constraint was used between the O_η and a suitable point on the target residue.

b These residues are conserved between GLP-1R and VPAC-2R. The restraint gives similar results for E^9 with K197 and/or R190; if the constraint is used with both residues it can be relaxed to $r_{AB} \leq 5.0$ Å or $r_{AB} \leq 6.0$ Å.

c The potential constraint between $O_{\varepsilon1}$ of E125 and C_α of G^{35} reported by Chen et al. 2009 was not used as the distance in the ECD X-ray structure is 21.5 Å; this is possibly a constraint to another molecule within an oligomeric array.

Table 2. ***Effects of human GLP-1 receptor mutation on peptide ligand binding and cell surface expression.***

Binding data were analysed using a three-parameter logistic equation as defined in Equation 1 to obtain pIC_{50} values. Data were normalised to maximum ^{125}I-exendin(9-39) binding in the absence of ligand, with nonspecific binding measured in the presence of 1 μM exendin(9-39). Cell surface expression (B_{max}) was determined through homologous competition binding with [^{125}I]exendin(9-39), and data are expressed as a maximum of specific [^{125}I]exendin(9-39) binding at the wildtype human GLP-1R. All values are expressed as mean ± S.E.M. of three to seven independent experiments, conducted in duplicate. Data were analysed with one-way analysis of variance and Dunnett's post-test.

	Binding (pIC_{50})				**Cell Surface Expression ELISA (% wildtype)**	**Cell Surface Expression (B_{max}) (% wildtype)**
	GLP-1(7-36)NH_2	Exendin-4	Oxyntomodulin	Exendin(9-39)		
Wildtype**	8.7 ± 0.1	9.0 ± 0.0	7.3 ± 0.1	8.1 ± 0.1	100 ± 1	100 ± 3
R2.60^{190}A**	**7.4 ± 0.1***	**7.3 ± 0.1***	7.6 ± 0.2	**7.6 ± 0.1***	**53 ± 3***	**44 ± 2***
N3.43^{240}A**	**8.2 ± 0.1***	8.7 ± 0.1	7.4 ± 0.1	8.3 ± 0.1	86 ± 3	92 ± 2
Q7.49^{394}A**	8.6 ± 0.1	8.8 ± 0.1	7.3 ± 0.2	8.2 ± 0.1	103 ± 3	111 ± 2
N3.43^{240}A/Q7.49^{394}A	**8.0 ± 0.1***	**8.1 ± 0.1***	7.4 ± 0.1	8.0 ± 0.1	**65 ± 4***	**71 ± 4***
N3.43^{240}Q	8.3 ± 0.1	8.8 ± 0.1	7.6 ± 0.1	8.3 ± 0.1	84 ± 6	**80 ± 7***
Q7.49^{394}N	8.7 ± 0.1	8.8 ± 0.1	7.4 ± 0.1	8.2 ± 0.1	98 ± 7	93 ± 5
N3.43^{240}Q/Q7.49^{394}N	8.4 ± 0.1	**8.6 ± 0.1***	7.3 ± 0.0	**7.7 ± 0.1***	88 ± 10	**80 ± 7***
E6.53^{364}A	**7.3 ± 0.1***	**7.5 ± 0.1***	7.1 ± 0.2	**7.5 ± 0.1***	**41 ± 4***	**51 ± 6***
H6.52^{363}A**	**7.3 ± 0.1***	**7.5 ± 0.1***	**6.5 ± 0.1***	**7.4 ± 0.1***	**59 ± 4***	**53 ± 2***

* Statistically significant at $p < 0.05$, one-way analysis of variance and Dunnett's post-test in comparison to wildtype control.

** Data obtained from Wootten et al., 2013a.

Table 3. ***Effects of human GLP-1 receptor mutation on agonist signaling.***

All mutants were analysed with an operational model of agonism (Equation 2) to determine logτ values. All logτ values were then corrected to Bmax values determined from homologous competition binding between ^{125}I-exendin(9-39) and unlabelled exendin(9-39) ($\log\tau_c$). Values are expressed as mean ± S.E.M. of four to six independent experiments, conducted in duplicate. Data were analysed with one-way analysis of variance and Dunnett's post-test.

	cAMP accumulation			**pERK1/2**			**$_i$Ca^{2+} mobilisation**		
	GLP-1 (7-36)NH_2	Exendin-4	Oxyntomodulin	GLP-1 (7-36)NH_2	Exendin-4	Oxyntomodulin	GLP-1 (7-36)NH_2	Exendin-4	Oxyntomodulin
	$\log\tau_c$	$\log\tau_c$	$\log\tau_c$	$\log\tau_c$	$\log\tau_c$	$\log\tau_c$	$\log\tau_c$	$\log\tau_c$	$\log\tau_c$
Wildtype	1.22 ± 0.11	1.33 ± 0.11	0.92 ± 0.16	-0.08 ± 0.03	-0.09 ± 0.03	-0.07 ± 0.03	-0.30 ± 0.00	-0.31 ± 0.03	-0.31 ± 0.02
R2.60^{190}A**	**0.53 ± 0.07***	**0.80 ± 0.08***	**1.56 ± 0.09***	**-0.39 ± 0.08***	**-0.51 ± 0.12***	0.03 ± 0.07	-0.66 ± 0.16	-0.72 ± 0.11	**0.11 ± 0.05***
N3.43^{240}A**	**0.55 ± 0.12***	1.46 ± 0.15	0.89 ± 0.10	0.01 ± 0.04	**0.19 ± 0.05***	0.04 ± 0.02	-0.76 ± 0.16	**-0.96 ± 0.10***	-0.29 ± 0.04
Q7.49^{394}A**	0.86 ± 0.11	1.16 ± 0.15	**0.41 ± 0.05***	**-0.54 ± 0.05***	-0.29 ± 0.05	-0.20 ± 0.01	**-1.12 ± 0.13***	**-1.13 ± 0.34***	**N.D.**
N3.43^{240}A/Q 7.49^{394}A	**0.52 ± 0.12***	1.07 ± 0.11	0.71 ± 0.12	**-0.56 ± 0.04***	**-0.43 ± 0.07***	-0.09 ± 0.03	**-1.11 ± 0.19***	**N.D.**	**N.D.**
N3.43^{240}Q	1.09 ± 0.13	1.15 ± 0.17	0.74 ± 0.07	-0.09 ± 0.04	-0.05 ± 0.03	-0.27 ± 0.04	**-0.80 ± 0.05***	-0.71 ± 0.10	**N.D.**
Q7.49^{394}N	0.91 ± 0.14	1.30 ± 0.13	**0.45 ± 0.09***	-0.09 ± 0.04	-0.05 ± 0.03	-0.10 ± 0.03	-0.70 ± 0.04	-0.67 ± 0.03	**-0.59 ± 0.07***
N3.43^{240}Q/Q 7.49^{394}N	0.75 ± 0.16	0.87 ± 0.15	**0.44 ± 0.10***	-0.06 ± 0.04	-0.00 ± 0.03	**-0.44 ± 0.06***	**-1.15 ± 0.10***	**-1.00 ± 0.14***	**N.D.**
E6.53^{364}A	**0.56 ± 0.07***	**0.85 ± 0.06***	1.10 ± 0.06	-0.35 ± 0.08	-0.37 ± 0.09	-0.11 ± 0.07	-0.38 ± 0.13	-0.68 ± 0.04	0.04 ± 0.05
H6.52^{363}A**	**-0.51 ± 0.11***	**-0.31 ± 0.06***	**-0.26 ± 0.06***	**-0.81 ± 0.15***	**-0.67 ± 0.07***	-0.19 ± 0.08	**-1.09 ± 0.13***	**-1.33 ± 0.22***	-0.23 ± 0.27

* Statistically significant at $p < 0.05$, one-way analysis of variance and Dunnett's post-test in comparison to wildtype control.

** Data obtained from Wootten et al., 2013a.

FIGURE 1

Molecular Pharmacology Fast Forward. Published on December 23, 2015 as DOI: 10.1124/mol.115.101246
This article has not been copyedited and formatted. The final version may differ from this version.

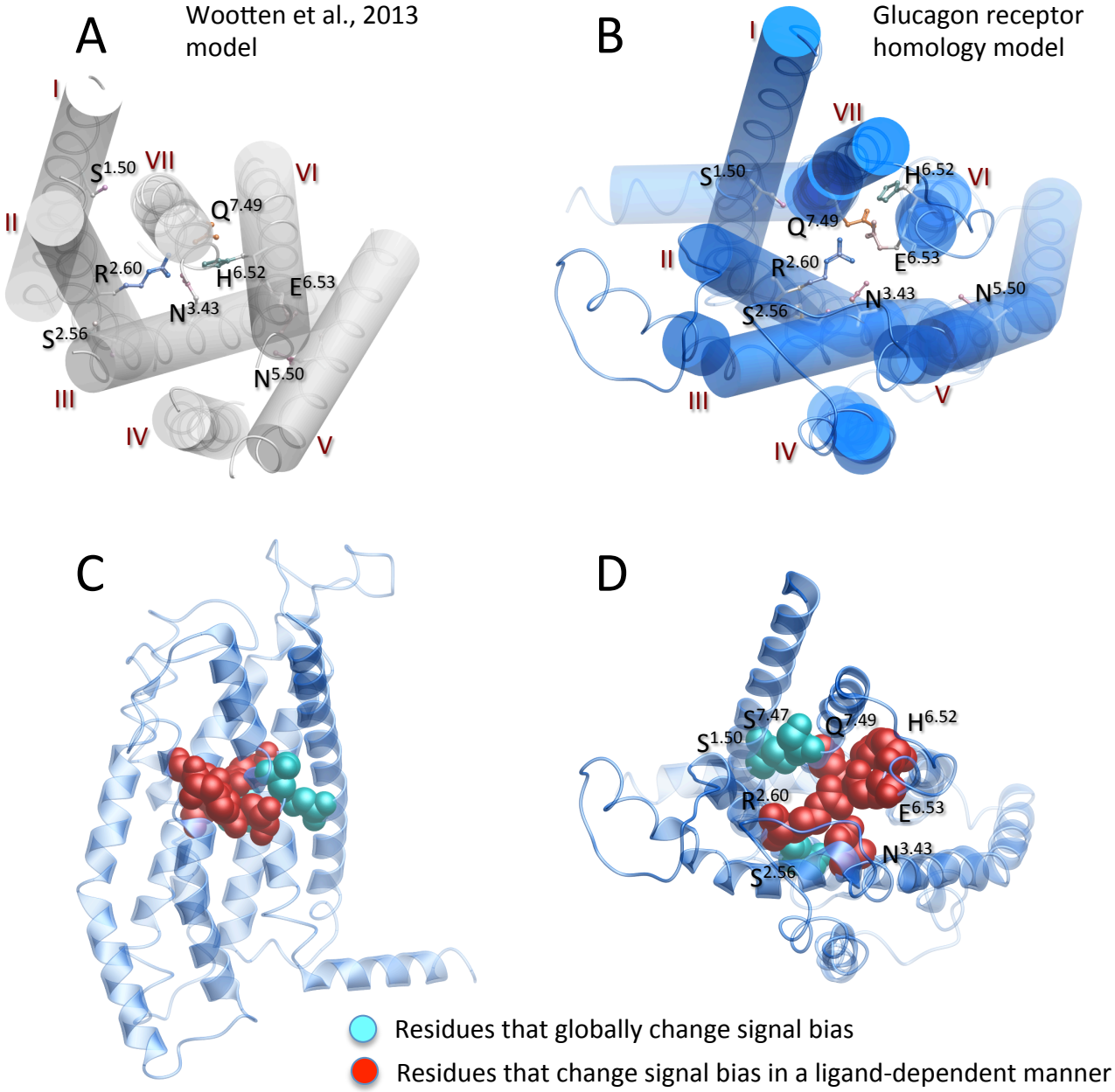

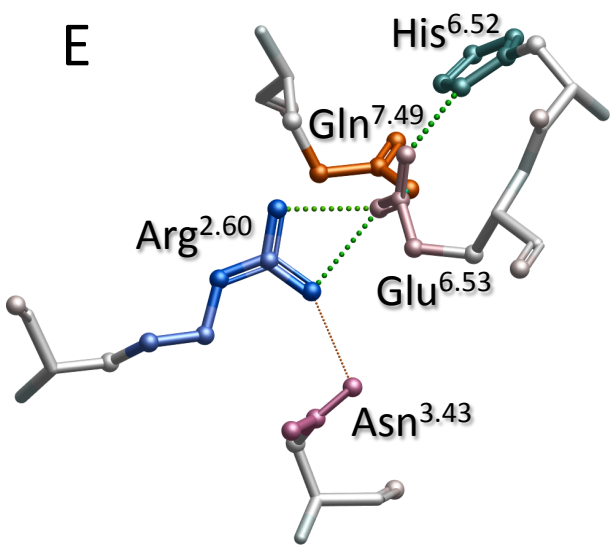

FIGURE 2

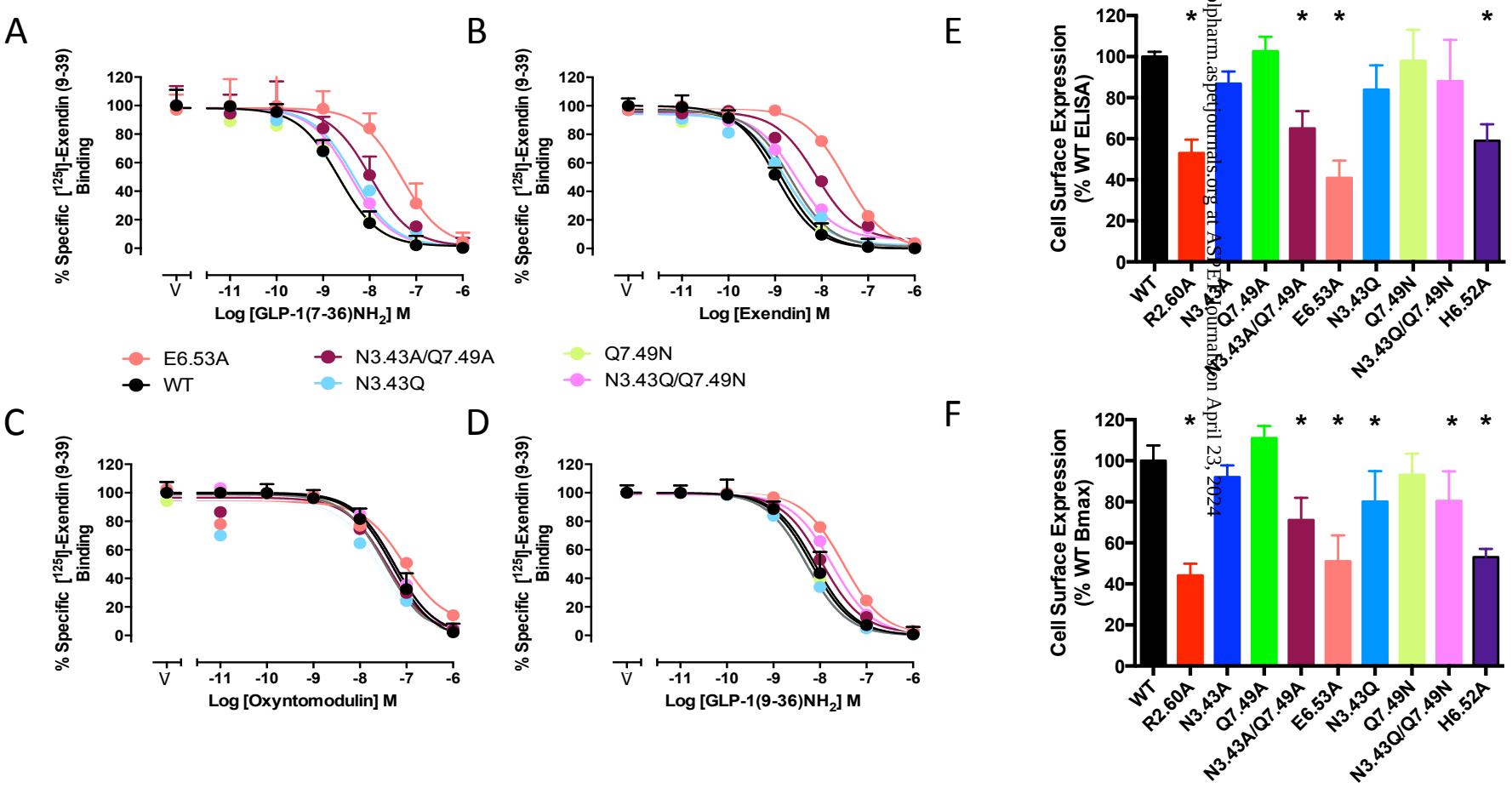

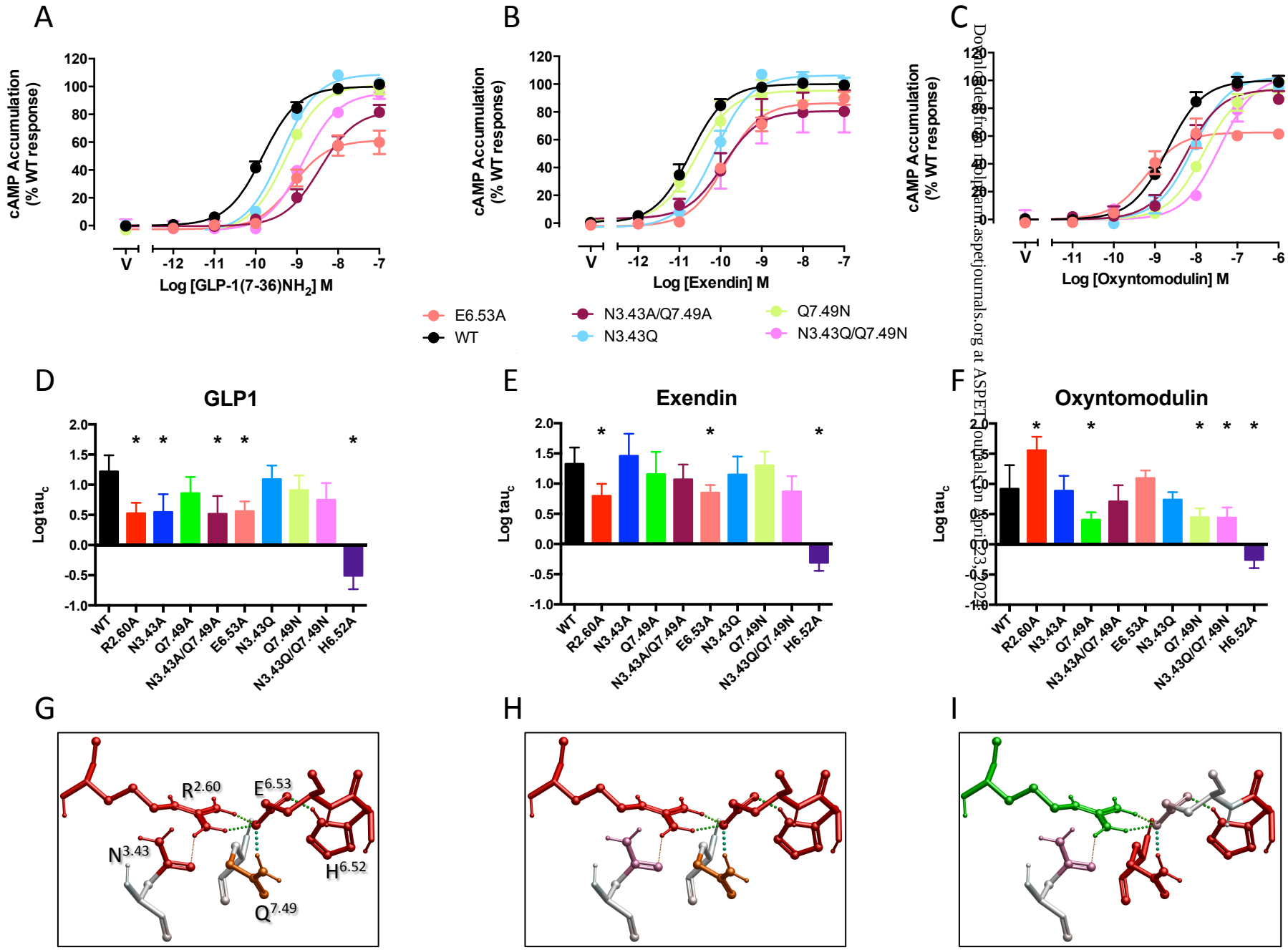

FIGURE 3

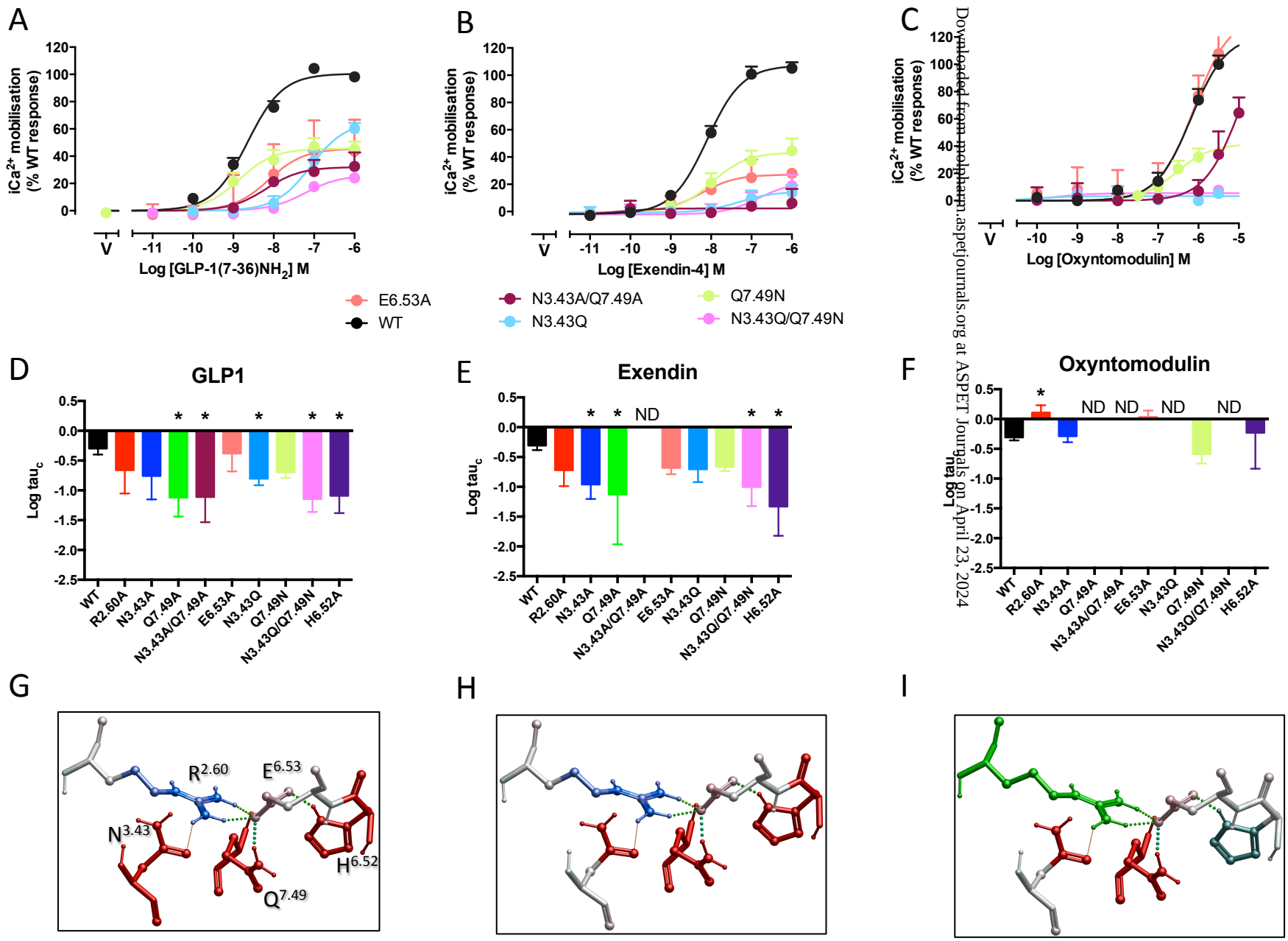

FIGURE 4

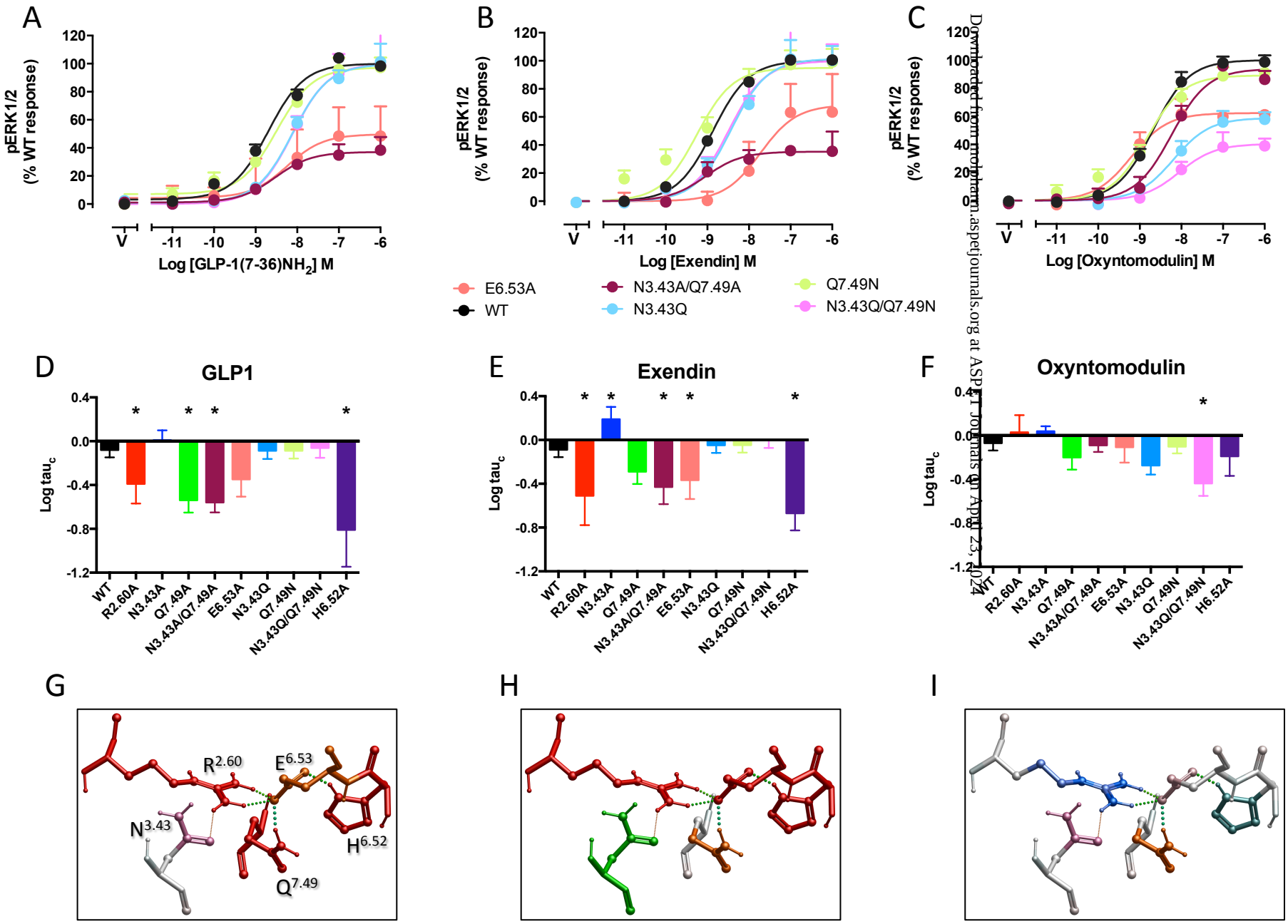

FIGURE 5

FIGURE 6

Molecular Pharmacology Fast Forward. Published on December 23, 2015 as DOI: 10.1124/mol.115.101246
This article has not been copyedited and formatted. The final version may differ from this version.

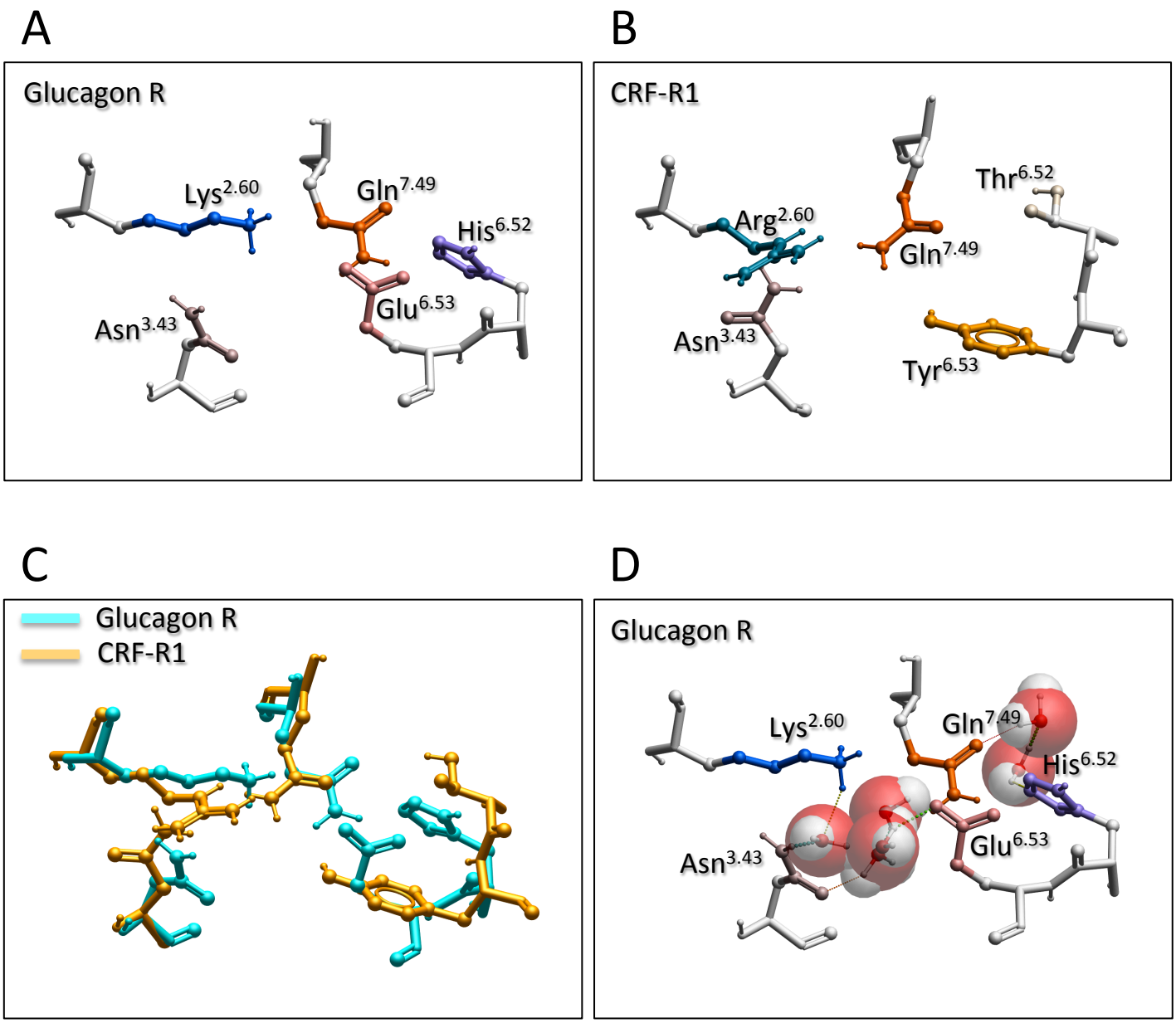

FIGURE 7

Molecular Pharmacology Fast Forward. Published on December 23, 2015 as DOI: 10.1124/mol.115.101246
This article has not been copyedited and formatted. The final version may differ from this version.